A&A 409, L31–L34 (2003)
DOI: 10.1051/0004-6361:20031339

Astronomy & Astrophysics

Optical identification of the companion to PSR J1911−5958A, the pulsar binary in the outskirts of NGC 6752

C. G. Bassa[1], F. Verbunt[1], M. H. van Kerkwijk[2], and L. Homer[3]

[1] Astronomical Institute, Utrecht University, PO Box 80 000, 3508 TA Utrecht, The Netherlands
[2] Dept. of Astronomy and Astrophysics, Univ. of Toronto, 60 St. George Street, Toronto, ON M5S 3H8, Canada
[3] Dept. of Astronomy, Univ. of Washington, Box 351580, Seattle, WA 98195-1580, USA

Received 17 July 2003 / Accepted 1 September 2003

Abstract. We report on the identification of the optical counterpart of the binary millisecond pulsar PSR J1911−5958A, located in the outskirts of the globular cluster NGC 6752. At the position of the pulsar we find an object with $V = 22.08$, $B - V = 0.38$, $U - B = -0.49$. The object is blue with respect to the cluster main sequence by 0.8 mag in $B - V$. We argue that the object is the white dwarf companion of the pulsar. Comparison with white dwarf cooling models shows that this magnitude and colors are consistent with a low-mass white dwarf at the distance of NGC 6752. If associated with NGC 6752, the white dwarf is relatively young, $\lesssim$2 Gyr, which sets constraints on the formation of the binary and its ejection from the core of the globular cluster.

Key words. pulsars: individual: PSR J1911−5958A – globular clusters: individual: NGC 6752 – stars: neutron – stars: white dwarfs

1. Introduction

Recently, 5 millisecond pulsars have been discovered (D'Amico et al. 2002) towards the nearby galactic globular cluster NGC 6752. Three of them are located inside the 6.′7 core radius (Lugger et al. 1995) while the other two are outside the 1.′92 half-mass radius (Djorgovski 1993), at 2.′7 and 6.′4, respectively. The latter of these is a binary millisecond pulsar, PSR J1911−5958A (hereafter PSR A), and has a low-mass ($\gtrsim$0.19 $M_\odot$, assuming a 1.4 $M_\odot$ neutron star) companion in a 20 hour, highly circular ($e < 10^{-5}$) orbit (D'Amico et al. 2002). The pulsar period and period derivative suggest that it is a "canonical" recycled millisecond pulsar (see Phinney & Kulkarni 1994 for a review), and hence that the companion is likely a white dwarf.

The large separation of PSR A from the cluster center is puzzling. Colpi et al. (2002) have recently investigated possible scenarios, and found that both for the case of a primordial binary and for an exchange or scattering event with other cluster stars, it is very difficult to explain both the pulsar's current position and its close circular binary orbit. Instead, they suggest that the binary may have been scattered to its current position by a binary composed of two 3–100 $M_\odot$ black holes.

One might learn more about the system's origin (and verify cluster membership) if one can confirm that the companion is a white dwarf and measure its mass and age. Therefore, we searched for the optical counterpart in archival data. We report here on the results.

Send offprint requests to: C. G. Bassa,
e-mail: c.g.bassa@astro.uu.nl

2. Observations and analysis

We searched the ESO and *Hubble Space Telescope* archives for images coincident with the pulsar position (α_{2000} = $19^h11^m42\overset{s}{.}7562$, δ_{2000} = −59°58′26.″900; D'Amico et al. 2002). We found two images, taken with the Wide Field Imager (WFI) at the ESO 2.2 m telescope on La Silla. These observations, 4 min B and V-band exposures, were taken during the night of May 13/14, 1999. The seeing was poor, ∼1.″5 in V. However, both images showed a faint object at the pulsar position (see below). This object was also present in two *HST* observations with the Wide Field Planetary Camera 2 (WFPC2; Holtzman et al. 1995). Both observations, `U5FI07` and `U5FI03` (GO-8256), were imaged in the same filters and had similar exposure times, 42 s in F555W (hereafter V_{555}), 220 s in F439W (B_{439}), 660 s in F336W (U_{336}) and 1 800 s and 1 693.5 s in F255W (nUV_{255}) for the first and second field, respectively. The position of the pulsar coincides with the WF3 chip for the `U5FI07` dataset, while it is on the WF4 chip on the other dataset.

2.1. Astrometry

The WFI detector has an array of 8 CCDs (2 rows of 4), each CCD having a field of view of 8′ × 16′, a total of 33′ × 34′. The position of the pulsar was coincident with chip 6 of the V-band

image. We found that there was some distortion over the whole chip. To minimize its effect we only used the upper half of this chip for the astrometric calibration. Stars on this $8' \times 8'$ sub-image were compared against entries in the USNO CCD Astrograph Catalog (UCAC; Zacharias et al. 2000). In total 68 UCAC stars coincided with this image and their centroids were measured. Of these 43 were not saturated and appeared stellar and unblended. One outlier, having a total residual of 0.″32 was rejected. The remaining stars were used to calculate an astrometric solution, fitting for zero-point position, scale and position angle. This solution has root-mean-square (rms) residuals of 0.″06 in both right ascension and declination. The statistical uncertainty in the astrometry is thus 0.″084 in each coordinate.

We used the astrometrically calibrated WFI image to obtain astrometric solutions for the two *HST*/WFPC2 datasets. First, the WFPC2 pixel positions were corrected for geometric distortion and placed on a master-frame, using the prescription of Anderson & King (2003). We matched stars on the WFI image and fitted for zero-point position, scale and position angle against the WFPC2 master frame positions. Outliers having residuals larger than three times the rms residual of the fit are removed and a new solution is computed. This process is iterated until convergence. On average the converged astrometric solution used some 200–300 stars with rms residuals of the order of 0.″03 in both right ascension and declination. The final uncertainty in the tie to the UCAC system is dominated by the step from the UCAC to the WFI sub-image, and is ∼0.″10 in each coordinate.

2.2. Photometry

We started with the pipe-line calibrated *HST*/WFPC2 images, and used the HSTphot 1.1 (Dolphin 2000a) package for further reduction and photometry of the images. We followed the recommended procedures to mask bad pixels, defects, cosmic ray hits and hot pixels. Next we used the main task *hstphot* to find stars, measure positions, and determine calibrated photometry. The latter uses the aperture corrections, charge-transfer efficiency corrections and zero-points of Dolphin (2000b).

2.3. The counterpart to PSR J1911−5958A

The UCAC catalog is on the ICRS at the 20 mas level (Assafin et al. 2003). Including this uncertainty in the uncertainty of the astrometric tie, we obtain 95% confidence radii for the WFI and *HST*/WFPC2 frames of 0.″211 and 0.″235, respectively. Within these radii there is a single object, see Fig. 1. The *HST*/WFPC2 positions and magnitudes are tabulated in Table 1.

The photometric measurements of the object in the two datasets are consistent for all filters except nUV_{255}. The object is 0.7 mag brighter in the first dataset than in the second. However, we compared the magnitudes of 240 stars that overlapped between the two datasets and found that, on average, stars in the first dataset were brighter by 0.34 mag in nUV_{255}, which removes the observed discrepancy. We have not, however, found an explanation for this large offset between the two datasets.

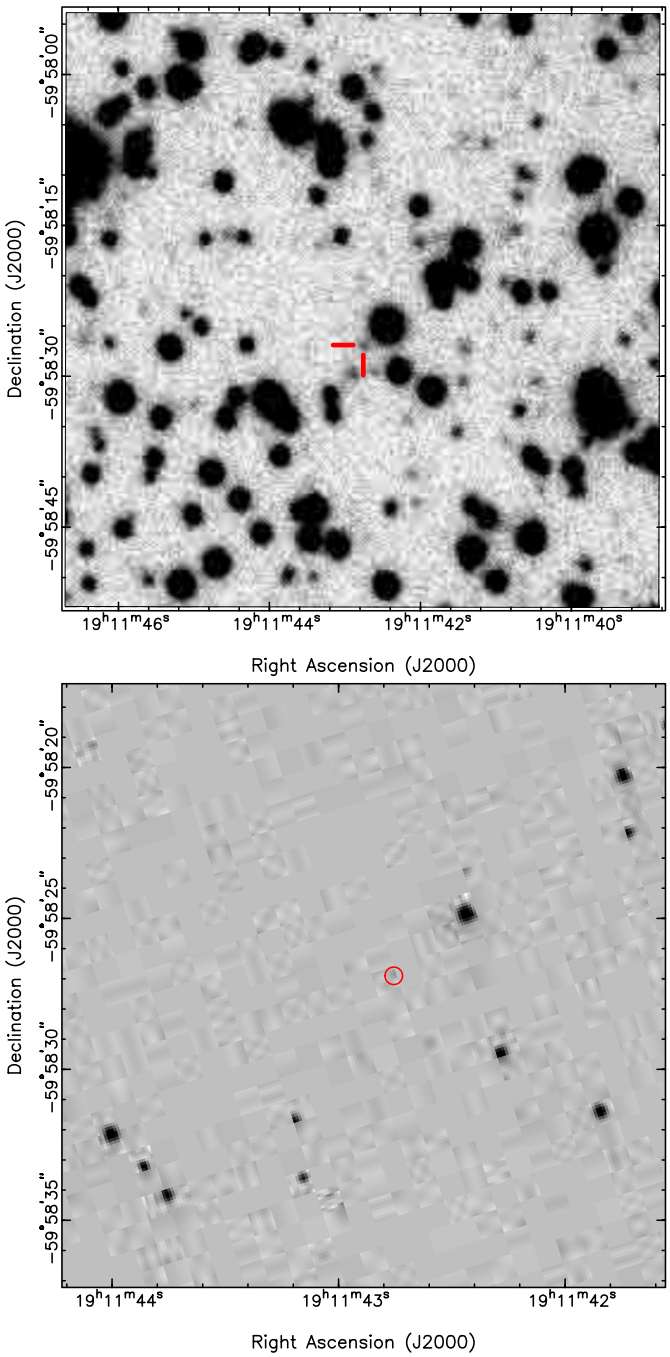

Fig. 1. Finding charts for PSR A. The upper image is a $1' \times 1'$ subsection of a *V*-band image obtained on May 14, 1999 with the Wide Field Imager on the ESO 2.2 m telescope at La Silla. The 2″ tick marks indicate the position of PSR A. The lower image is a $20'' \times 20''$ sub-image of the *HST*/WFPC2 V_{555} (F555W) observation. The 0.″235 (95% confidence) error circle is shown at the position of the pulsar.

The magnitudes in the *HST* flight system filters (U_{336}, B_{439} and V_{555}) were transformed to the Johnson-Cousins *UBV* (Vega) system using the transformations by Holtzman et al. (1995). The resulting average magnitudes for the object in this system are $U = 21.96 \pm 0.10$, $B = 22.46 \pm 0.14$ and $V = 22.08 \pm 0.11$. The object is blue by about 0.8 mag with

Table 1. Positional and photometric data.

Dataset	Date (UT)	RA (J2000)	Decl. (J2000)	nUV_{255}	U_{336}	B_{439}	V_{555}
U5FI07	March 2, 2000 @ 10:29	$19^h11^m42\overset{s}{.}756$	$-59°58'26\overset{''}{.}87$	20.74 ± 0.23	21.49 ± 0.15	22.40 ± 0.21	22.10 ± 0.17
U5FI03	March 3, 2000 @ 13:54	$19^h11^m42\overset{s}{.}757$	$-59°58'26\overset{''}{.}83$	21.44 ± 0.24	21.78 ± 0.14	22.49 ± 0.17	22.09 ± 0.14

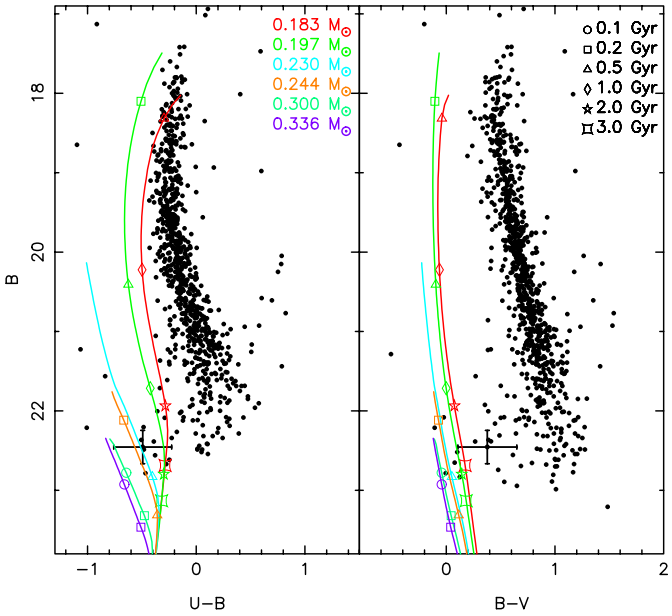

Fig. 2. Color–magnitude diagrams of the two *HST*/WFPC2 fields. The magnitudes are transformed from the *HST*/WFPC2 flight system to Johnson-Cousins *UBV* using the prescription by Holtzman et al. (1995). The average colors and magnitudes of the counterpart to PSR A are indicated with error bars. The errors include the uncertainty in the distance modulus and reddenning. Also shown are helium–core white dwarf cooling tracks (solid lines) by Serenelli et al. (2002). The models have masses of 0.183, 0.197, 0.230, 0.244, 0.300 and 0.336 $M_\odot$, decreasing in mass to the red, for a metallicity of $Z = 0.001$. The age of the white dwarfs along the cooling track is indicated.

respect to the cluster main sequence in $B-V$ at the same B-band magnitude, Fig. 2. This is also confirmed by an instrumental color-magnitude diagram constructed from the WFI B and V-band images.

Given the density of objects on the *HST*/WFPC2 chips, there is a ∼1% probability of a chance coincidence in the 95% confidence *HST* error circle. However, there are only a few stars that are blue with respect to the cluster main sequence, which greatly reduces the probability of a chance coincidence. The blue color, together with the positional coincidence, gives us confidence that we have detected the companion of PSR A.

3. Ramifications

The minimum mass for the companion is constrained by the pulsar mass function. For a pulsar mass of 1.35 $M_\odot$ (Thorsett & Chakrabarty 1999) this minimum mass is 0.185 $M_\odot$. The lower limit increases for heavier pulsars, roughly by 0.004 $M_\odot$ for every 0.05 $M_\odot$ step in the pulsar mass. Assuming a random probability distribution for the inclination of the binary, we find that there is 90% probability that the companion mass is less than 0.5 $M_\odot$. Given this range of masses and the fact that PSR A is a recycled millisecond pulsar, it is likely that the companion is a helium-core white dwarf.

To verify whether our observations are compatible with a helium-core white dwarf at the distance of the cluster, we compare our magnitudes with the predictions from the white dwarf cooling tracks of Serenelli et al. (2002). We use their tracks for $Z = 0.001$, as this metallicity provides the best match to the metallicity of NGC 6752 ([Fe/H] = −1.43 ± 0.04; Gratton et al. 2003). We also assume a V-band distance modulus $(m - M)_V = 13.24 \pm 0.08$ and reddening $E_{B-V} = 0.040$, as recently determined by Gratton et al. (2003), and use the relative extinction coefficients listed by Schlegel et al. (1998).

Figure 2 shows the cooling tracks for helium-core white dwarfs with $Z = 0.001$ for masses in the range of 0.183 to 0.336 $M_\odot$. It appears that the magnitude and colors of the companion to PSR A are compatible with the two lowest-mass tracks, 0.183 and 0.197 $M_\odot$. Note that the 0.183 $M_\odot$ model is below the minimum mass inferred from the pulsar mass function.

We have fitted the observed absolute *UBV* magnitudes against the predictions from the $Z = 0.001$ helium-core white dwarf models. A χ^2 statistic was computed for each entry in the model from the difference between the observed and modelled absolute magnitudes. Table 2 shows, for each model with a given mass, the properties of the white dwarf at the χ^2 minimum. Both Fig. 2 as Table 2 show that the lowest mass models, 0.197 to 0.244 $M_\odot$, are preferred. At these masses the white dwarf is rather hot, with $T_{\rm eff} \approx 11\,000$–$16\,000$ K.

Given these high temperatures, the counterpart is relatively young, $\lesssim$2 Gyr (see both Fig. 2 and Table 2). The precise value strongly depends on the mass, since white dwarfs with lower masses have relatively thick hydrogen envelopes, where residual hydrogen shell burning keeps the white dwarf hot. From the values listed in Table 2, one sees a jump in the cooling age between the 0.197 and 0.230 $M_\odot$ models. This reflects a dichotomy in the thickness of the hydrogen layer, where, above a certain critical mass, the thickness has been reduced by shell flashes early in the evolution (Althaus et al. 2001). As the shell burning is through the CNO cycle, the critical mass depends on the metallicity: ∼0.18 $M_\odot$ for solar metallicity, ∼0.22 $M_\odot$ for $Z = 0.001$ and ∼0.26 $M_\odot$ for $Z = 0.0002$ (Althaus et al. 2001; Serenelli et al. 2002).

We should note that the dichotomy in cooling age was not found by Driebe et al. (1998), who found the flashes hardly affected the thickness of the hydrogen layer. As a result, more massive white dwarfs cool slower and are older. However, for the mass range of interest here, their results are

Table 2. Fitting results for helium–core white dwarf models with a metallicity of $Z = 0.001$. The observed absolute UBV magnitudes were fitted against the modelled values. The dereddened, observed values $U - B$, $B - V$ and M_V are given in the second row.

Mass ($M_\odot$)	$T_{\rm eff}$ (kK)	τ_c (Gyr)	$(U-B)_0$ −0.54	$(B-V)_0$ 0.34	M_V 8.84	χ^2_ν
0.183	10.6	2.30	−0.31	0.08	8.92	0.9
0.197	11.7	1.36	−0.37	0.03	8.98	1.1
0.230	14.7	0.37	−0.59	−0.06	9.14	3.4
0.244	15.6	0.27	−0.64	−0.08	9.18	4.2
0.300	19.1	0.07	−0.80	−0.13	9.29	8.1
0.336	20.3	0.05	−0.85	−0.14	9.33	9.5
0.380	21.6	0.05	−0.89	−0.16	9.34	10.6
0.390	22.1	0.04	−0.91	−0.16	9.34	11.1
0.422	23.8	0.03	−0.95	−0.18	9.39	12.9
0.449	24.7	0.06	−0.98	−0.19	9.40	13.7

similar. Their 0.195 $M_\odot$ model has a cooling age of 1.2 Gyr, comparable to the age of the Serenelli 0.197 $M_\odot$ model. For higher masses the cooling age decreases. The 0.300 $M_\odot$ model by Driebe et al. (1998) has a cooling age of 0.2 Gyr, down to 25 Myr for the heaviest model, with a mass of 0.414 $M_\odot$.

Finally, we note the similarity between the position in the color-magnitude diagram of the companion of PSR A and the companion of PSR J0024−7204W (Edmonds et al. 2002) in 47 Tucanae. On the basis of optical variability with the orbital period (3.2 h) and eclipses of the pulsar radio emission, the companion is argued to be a heated main sequence star. For PSR A, however, we can exclude this possibility: the spin-down luminosity is too low to lead to heating to the observed temperature.

4. Discussion and conclusions

We have detected the optical companion to the binary millisecond pulsar PSR J1911−5958A, which is located 6.′4 from the center of NGC 6752. The companion is blue with respect to the cluster main sequence by 0.8 mag in $B - V$ and comparison of its colors and magnitude with white dwarf models shows that it is consistent with a helium-core white dwarf at the distance of NGC 6752.

Irrespective of the cooling models we use, we find that the white dwarf is at most 2 Gyr old. This age is similar to the $\gtrsim$0.7 Gyr the binary can be expected to stay in the outskirts if it is currently on a highly eccentric orbit in the cluster (Colpi et al. 2002), which suggests that the white dwarf formed during, or shortly after, an encounter that also ejected the binary from the core, in an exchange interaction involving a binary with another star or binary. In the scenarios in which the binary was formed in the periphery, or scattered by a binary black hole, the coincidence of the two time scales has to be due to chance.

One would expect the characteristic age of the pulsar to be similar to the cooling age of the white dwarf, as the pulsar starts to spin down after the cessation of mass transfer, while the white dwarf starts to cool. This seems not to be the case for PSR A, for the characteristic age of the pulsar is $P/(2\dot{P}) \sim 17$ Gyr (D'Amico et al. 2002). It may be instead that the assumption underlying the characteristic age is wrong, and that the period at which the pulsar started spinning is similar to the current one.

Compared to other white dwarf companions to millisecond pulsars, the companion to PSR J1911−5958A is bright, $V \simeq 22$, which opens the possibility to determine detailed physical parameters (e.g., Van Kerkwijk et al. 1996; Callanan et al. 1998). For instance, one could measure the white dwarf temperature and surface gravity through spectroscopy. By comparison with models, this would lead to a mass and radius of the white dwarf, as well as a much more precise cooling age. The radius would allow one to confirm the association of the binary with NGC 6752. If the association is confirmed, the more accurate distance to NGC 6752 provides additional constraints on the radius and thus the mass of the white dwarf. Combining the white dwarf mass with a radial-velocity orbit of the white dwarf (and thus a mass ratio), would give the mass of the pulsar.

Acknowledgements. This research is based on observations made with the European Southern Observatory telescopes obtained from the ESO/ST-ECF Science Archive Facilities and observations made with the NASA/ESA *Hubble Space Telescope*, obtained from the data archive at the Space Telescope Institute. STScI is operated by the association of Universities for Research in Astronomy, Inc. under NASA contract NAS 5-2655. CGB is supported by the Netherlands Organization for Scientific Research.

References

Althaus, L. G., Serenelli, A. M., & Benvenuto, O. G. 2001, MNRAS, 324, 617
Anderson, J., & King, I. R. 2003, PASP, 115, 113
Assafin, M., Zacharias, N., Rafferty, T. J., et al. 2003, AJ, 125, 2728
Callanan, P. J., Garnavich, P. M., & Koester, D. 1998, MNRAS, 298, 207
Colpi, M., Possenti, A., & Gualandris, A. 2002, ApJ, 570, L85
D'Amico, N., Possenti, A., Fici, L., et al. 2002, ApJ, 570, L89
Djorgovski, S. 1993, Structure and Dynamics of Globular Clusters, ed. S. G. Djorgovski, & G. Meylan (San Francisco: ASP), ASP Conf. Ser., 50, 373
Dolphin, A. E. 2000a, PASP, 112, 1383
Dolphin, A. E. 2000b, PASP, 112, 1397
Driebe, T., Schönberger, D., Blöcker, T., & Herwig, F. 1998, A&A, 339, 123
Edmonds, P. D., Gilliland, R. L., Camilo, F., Heinke, C. O., & Grindlay, J. E. 2002, ApJ, 579, 741
Gratton, R. G., Bragaglia, A., Carretta, E., et al. 2003, A&A, 408, 529
Holtzman, J., Hester, J. J., Casertano, S., et al. 1995, PASP, 107, 156
Holtzman, J. A., Burrows, C. J., Casertano, S., et al. 1995, PASP, 107, 1065
Lugger, P. M., Cohn, H. N., & Grindlay, J. E. 1995, ApJ, 439, 191
Phinney, S. E., & Kulkarni, S. R. 1994, ARA&A, 32, 591
Schlegel, D. J., Finkbeiner, D. P., & Davis, M. 1998, ApJ, 500, 525
Serenelli, A. M., Althaus, A. G., Rohrmann, R. D., & Benvenuto, O. G. 2002, MNRAS, 337, 1091
Thorsett, S. E., & Chakrabarty, D. 1999, ApJ, 512, 288
Van Kerkwijk, M. H., Bergeron, P., & Kulkarni, S. R. 1996, ApJ, 467, L89
Zacharias, N., Urban, S. E. Zacharias, I. M., et al. 2000, AJ, 120, 2131